Pergamon

Available online at www.sciencedirect.com
SCIENCE DIRECT®

Cement and Concrete Research 34 (2004) 581–586

CEMENT AND CONCRETE RESEARCH

Amorphisation mechanism of a flint aggregate during the alkali–silica reaction: X-ray diffraction and X-ray absorption XANES contributions

J. Verstraete[a], L. Khouchaf[a,*], D. Bulteel[a], E. Garcia-Diaz[a], A.M. Flank[b], M.H. Tuilier[c]

[a]*Centre de Recherche de l'Ecole des Mines de Douai, 941, rue Charles Bourseul BP.34 59508, Douai, France*
[b]*Laboratoire pour l'Utilisation du Rayonnement Electromagnétique, LURE, Bât 209D BP.34 91898 91405, Orsay Cedex, France*
[c]*Equipe de Recherche Technologique, Université de Haute-Alsace, 61 rue Albert Camus, F-68093, Mulhouse Cedex, France*

Received 18 December 2002; accepted 11 September 2003

Abstract

Flint samples at different stages of the Alkali–Silica Reaction were prepared and analyzed by X-ray diffraction (XRD) and silicon K-edge X-ray absorption near edge structure techniques (XANES). The results are compared to those of measurements performed on alpha quartz c-SiO_2 and rough flint aggregate. The molar fraction of Q_3 sites is determined as a function of the time of reaction. Up to 14 h of attack, the effect of the reaction seems of little importance. From 30 to 168 h, we showed an acceleration of the effect of the reaction on the crystal structure of the aggregate resulting in an amorphisation of the crystal. During this period, the amorphous fraction increases linearly with the number of Q_3 sites. The results of the XANES confirm the amorphisation of the aggregate during the reaction and show the presence of silicon in a tetrahedral environment of oxygen whatever the time of attack.

Keywords: X-ray diffraction; Spectroscopy; Alkali–silica reaction; Aggregate; Degradation

1. Introduction

The alkali–silica reaction (ASR) is one of the causes that takes part in the degradation of the aggregate in concrete. Several assumptions are proposed to explain the origins and the mechanisms of the alkali silica reaction and its role in the degradation of the concrete [1,2]. The reactivity of an aggregate in a concrete depends on its degree of crystallinity. Accurate information on the structure of the aggregate is needed at the different stages of the ASR for a better knowledge of the concrete behavior [3]. Generally, we consider that the swelling phenomenon is induced by the formation of an ASR gel at the interface between the aggregate and the cement pastes [1,4,5] whose chemical composition can vary. Calcium- and alkali-enriched gels are observed [6]. In more recent papers [7,8], the swelling is attributed to the formation of an internal silica gel in the aggregate. This "internal" product appears like an amorphous product in optical microscopy and in environmental scanning electron microscope [9].

In order to observe the structural behavior of the aggregate during the ASR, we propose an approach using two techniques: X-ray diffraction (XRD) and X-ray absorption near-edge structure spectroscopy (XANES). Unlike X-ray diffraction, XANES can be used both for crystalline and amorphous materials and gives information on long- and short-range order. The XANES spectra are a good fingerprint of the degree of crystallinity in the sample [10–12]. It has been established that the various energy resonance above the edge are a signature of the presence of four- or sixfold environments for silicon atoms. Moreover, it has been indicated that the hydroxyl ions are chemisorbed onto the silica surface, increasing the coordination number of the silicon to more than four [2,13]. Studies of the crystal structure of materials containing SiO2 are numerous [14–16]. Li et al. [14,15] showed the interest of the XANES technique to follow-up the amorphisation in compounds containing SiO2 and contributed to the interpretation of the structures observed in the Si XANES spectra of various silicates. In a recent study, we have shown that XRD is well

* Corresponding author. Tel.: +33-3-37-71-23-19; fax: +33-3-27-71-23-18.
E-mail address: khouchaf@ensm-douai.fr (L. Khouchaf).

0008-8846/$ – see front matter © 2004 Elsevier Ltd. All rights reserved.
doi:10.1016/j.cemconres.2003.09.012

suited to study the evolution of the crystal structure of the flint aggregate during the reaction [3]. The aim of this study is to follow the structural evolution of a flint aggregate during the ASR. The methodology used consists in establishing a relationship between the structural parameters deduced from XRD, chemical parameters such as reaction degrees, and XANES studies.

2. Chemical mechanisms of alkali–silica reaction

2.1. Chemical mechanisms

The ASR mechanism was described using different models [1,4,5,17,18] and can be written following two main steps:

-Formation of Q_3 sites (Step 1) due to a first breaking up of siloxane bonds by hydroxide ions attack:

$$2SiO_2 + OH^- \rightarrow SiO_{5/2}^- + SiO_{5/2}H \quad (1)$$

Here, on a structural point of view, SiO_2 represents Q_4 silicon tetrahedron sharing four oxygen with four neighbors and using a simplified notation, $SiO_{5/2}^-$ represents the Q_3 (so-called "silanol" sites) negatively charged in a basic solution.

-Dissolution of silica (Step 2) due to continued hydroxide ions attack on the Q_3 sites to form silica ions:

$$SiO_{5/2}^- + OH^- + \frac{1}{2}H_2O \rightarrow H_2SiO_4^{2-} \quad (2)$$

These silica ions respect the Iler [19] equilibrium:

$$H_2SiO_4^{2-} + H_2O \Leftrightarrow H_3SiO_4^- + OH^- \quad (3)$$

Afterwards, precipitation of silica ions by the cations of the pore solution of concrete is likely to induce C-S-H and/or C-K-S-H phases formation:

$$H_2SiO_4^{2-} + Ca^{2+} + xH_2O \rightarrow C-S-H \quad (4)$$

$$2H_2SiO_4^{2-} + Ca^{2+} + 2K^{2+} + yH_2O \rightarrow C-K-S-H \quad (5)$$

2.2. Determination of reaction degrees

The development of our chemical method to quantify ASR enables the measurement of the dissolution degree α and the molar fraction of Q_3 sites n^* of Eqs. (1) and (2), which are defined as follows:

-dissolution degree: α

$$\alpha = \frac{\text{moles of dissolved silica}}{\text{moles of initial silica}} \quad (6)$$

-molar fraction of Q_3 sites: n^*

$$n^* = \frac{\text{moles of } Q_3 \text{ sites}}{\text{moles of residual silica}} \quad (7)$$

3. Experimental methods

3.1. Material

The material used is a flint aggregate from the north of France. X-ray fluorescence analysis gives a SiO_2 content close to 99%, and X-ray diffraction detects only quartz in this aggregate [3].

The flint crystal lattice has been characterized by crossed polarization ^{29}Si solid NMR spectroscopy [9]. This lattice is constituted of SiO_2 Q_4 tetrahedra (peak at -108 ppm) and Q_3 $SiO_{5/2}H$ "silanol" tetrahedra (peak at -99 ppm). The initial active sites ratio in the aggregate measured by thermogravimetric analysis was close to 0.08 moles of Q_3 active sites by moles of initial silica.

3.2. Sample preparation

We use a model reactor method developed by Bulteel et al. [8]. This method uses the following protocol organized in different stages:

-Initial stage: A mix of 1 g of crushed flint and 0.5 g of $Ca(OH)_2$ is introduced in a closed stainless steel container. After 30 min of preheating, 10 ml KOH solution of 0.79 mol/l are added. The mix is then autoclaved in an oven to develop ASR under controlled temperature and reaction time.

-Stage 1: After the reaction, the flint is constituted by Q_4 tetrahedra of the remaining silica, which did not react (sound silica) and by the Q_3 sites $SiO_{5/2}^-$, whose negative charges are balanced by cations (altered silica). The reactor also contains reaction products and reagents.

-Stage 2: The soluble reaction products K^+, Ca^{2+}, $H_2SiO_4^{2-}$, the C-S-H, C-K-S-H, and $Ca(OH)_2$ phases are removed by selective acid treatment and filtration. The acid attack is done using 250 ml cold 0.5M HCl solution. The remaining solid is composed of the remaining Q_4 tetrahedrons and of the protonated silanol Q_3 sites $SiO_{5/2}H$.

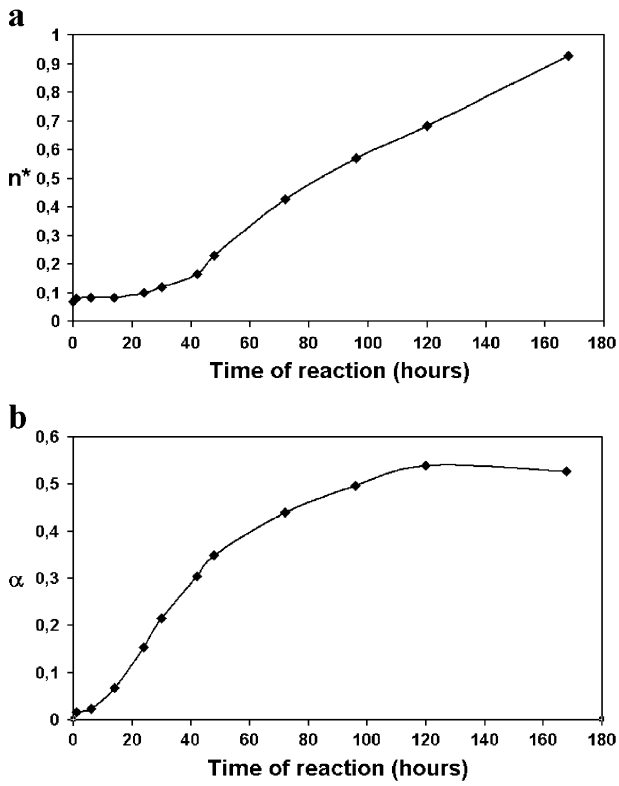

Fig. 1. (a) Evolution of the molar fraction of Q_3 sites n^* as a function of the duration of the alkali–silica reaction. (b) Evolution of dissolution degree α versus the duration of the alkali–silica reaction.

The samples are dried by acetone and diethyl ether treatment after the filtration, then kept inside dried atmosphere and without CO_2.

3.3. X-ray diffraction

XRD patterns were measured using a D8 Bruker horizontal diffractometer operating at 40 kV and 40 mA with Co radiation ($\lambda \approx 1$, 78,897 Å). A position-sensitive detector (PSD) has been employed. Data were recorded in reflexion between 17° and 100° in 2θ with a step size of 0.007° and a counting time of 10 s/step.

3.4. X-ray absorption

XANES experiments were carried out at the SA32 beam line of the SUPERACO ring at the LURE synchrotron radiation facility, Orsay, France with a stored electron energy of 800 MeV. Data at the Si K absorption edge (1839 eV) were collected in the total electron yield (TEY) mode from 1830 to 1910 eV, using 0.2 eV step. The beam was monochromatized by a double-crystal monochromator, equipped with two InSb single crystals. Crystalline silicon oxide (c-SiO2) was used as reference compound. Experiments were performed under vacuum (10^{-5} Torr).

4. Results

In order to follow the evolution of the structural behavior of the aggregate and to associate it to the molar fraction of Q_3 sites n^* and α, we studied by XRD and XANES the samples named 6, 14, 30, 72, and 168 h of reaction (for example, 14 h corresponds to the starting flint aggregate attacked during 14 h). Fig. 1a and b show, respectively, the evolution of n^* and α versus the duration of the alkali–silica reaction.

4.1. Evolution of n^* and dissolution degree α

The molar fraction of Q_3 silanol as a function of time is given in Fig. 1a. After a short plateau, about 14 h long, n^* increases with the reaction time. The increase of Q_3 silanol fraction with the time of attack shows that the Eq. (1) of Q_3 sites creation prevails on the Eq. (2) of Q_3 sites dissolution.

The dissolution degree α versus time, given in Fig. 1b, describes three steps. The first is a short plateau, about 6 h long. The second step is an increase in α between 6 and 120 h. During this step, the aggregates silica (SiO_2) degradation by ASR produces active sites $SiO_{5/2}^{-}$, which are dissolved to give $H_2SiO_4^{2-}$. The third step is an asymptote where α reaches about 0.54 after 120 h. This high proportion of finally dissolved silica shows that Eq. (2) plays an important part in this experiment where initial hydroxide ions concentration is high. This proportion of finally dissolved silica increases when hydroxide ions concentration increases [3].

4.2. X-ray diffraction

4.2.1. Validation of the method with standards

Thanks to X-ray diffraction, we are able to determine in a semiquantitative way the evolution of the amorphous fraction during the reaction. In order to validate our procedure, we studied the evolution of the quantity of the amorphous fraction in standards constituted by a mixture of c-SiO_2 and amorphous silica with various contents of amorphous silica (96%, 80%, 50%, 30%, 20%, and 7%). Fig. 2 shows the

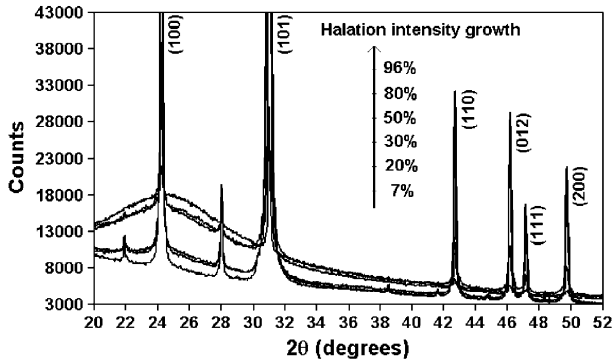

Fig. 2. X-ray diffraction patterns of reference compounds showing the evolution of the vitreous halation [λ(CoKα1) ≈ 1, 78,897 Å].

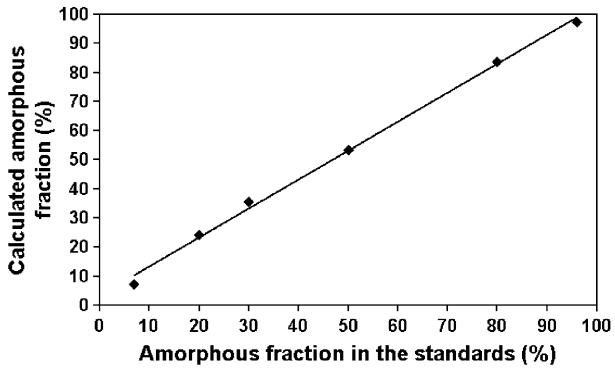

Fig. 3. Calculated amorphous fraction of silica by XRD versus the amorphous silica in the standards.

evolution of the XRD patterns in the different samples. One can notice the appearance of a vitreous halation in the zone located between 20° and 29° in 2θ, whose intensity increases with the content of amorphous silica (Fig. 2).

This increase corresponds a decrease in the intensity of the X-ray diffraction. The FWHM remains the same whatever the weight of the amorphous fraction. The amorphous fraction is obtained by calculating the areas of the X-ray diffraction peaks (Fig. 3) using the "DIFFRACPLUS" software of the Socabim [20]. From a semiquantitative point of view, we can consider that the agreement between the introduced values and those calculated is satisfactory. This correlation is much better when the amorphous percentage of silica is high.

4.2.2. ASR Samples

We used the same procedure to determine the amorphous fraction in the samples attacked during 6, 14, 30, 72, and 168 h of reaction as well as in rough flint. c-SiO_2 is taken as a reference to estimate the instrumental background noise and that related to absorption. Fig. 4 shows the evolution of the XRD patterns in the various samples compared to rough flint. A decreasing intensity of the diffraction peaks as well as an increase in the vitreous halation is observed. These evolutions are a good parameter to follow the change of the crystal structure of flint during the attack.

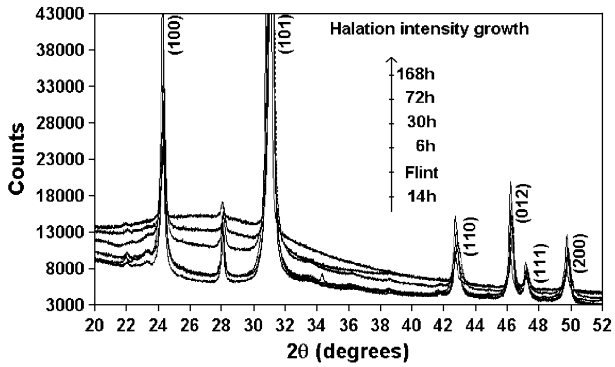

Fig. 4. X-ray diffraction patterns of the samples 6, 14, 30, 72, and 168 h compared to rough flint aggregate.

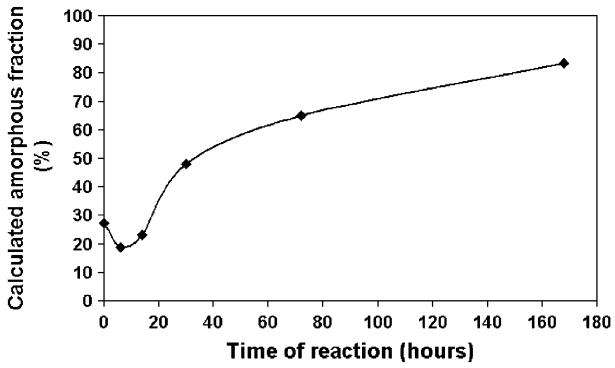

Fig. 5. Calculated amorphous fraction by XRD versus the duration of the alkali–silica reaction.

Fig. 5 represents the evolution of the amorphous fraction versus the time of attack. One can notice a decrease in the amorphous fraction at the beginning of the reaction up to 6 h, then it increases progressively until 14 h. It keeps increasing with the reaction time after 14 h and continues to increase until 168 h. It is significant to note that after 168 h of attack, the amorphisation of the aggregate is not complete. Fig. 6 represents the evolution of the amorphous fraction during the reaction versus n^*. Until 14 h of attack, one can note that the evolution remains weak. Then, we notice a quasi-linear increase in the amorphous fraction versus n^* especially from 30 h.

4.3. XANES characterization

In order to probe the local environment around silicon atoms, XANES was used at the Si K-edge. The Fig. 7a shows the evolution of XANES spectra of c-SiO_2 and rough flint. The main peaks are noted A, B, C, and D. The origin of these peaks is described in the literature [14,15]. One can note that XANES spectra of both compounds have almost the same structure with a weak decrease in the intensity of the flint spectrum.

We can also observe that the position of peak A located at 1847 eV is the same in both cases. The Fig. 7b represents XANES spectra of the samples obtained after 6, 14, 30, 72,

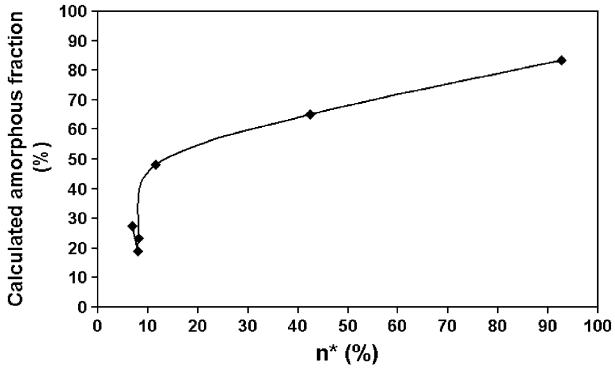

Fig. 6. Calculated amorphous fraction by XRD as a function of the molar fraction of Q_3 sites n^*.

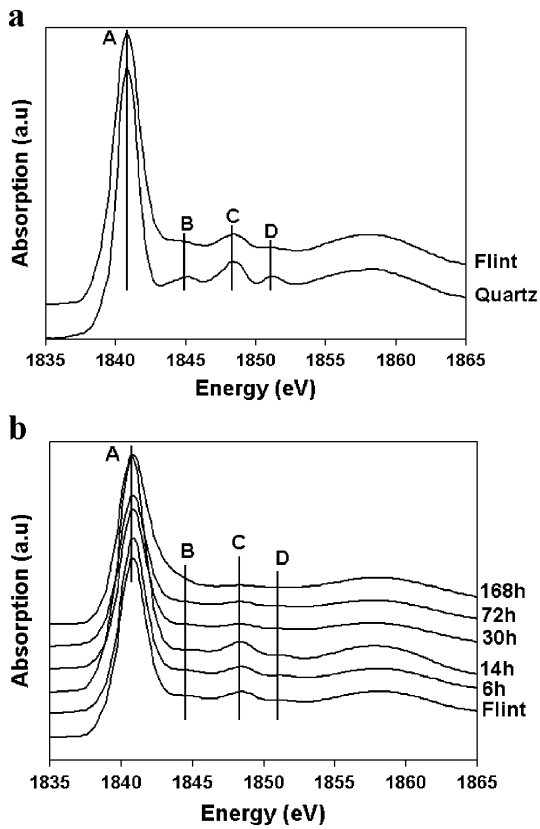

Fig. 7. (a) Si-K XANES spectra of c-SiO_2 and rough flint aggregate. (b) Si-K XANES spectra of the samples 6, 14, 30, 72, and 168 h compared to rough flint aggregate.

and 168 h of reaction compared to rough flint aggregate. We notice a decreasing intensity of the spectra of the samples during the reaction especially for B, C, and D peaks. As before, the position of A peak remains the same whatever the time of attack.

5. Discussion

To discuss the relationship among XRD, reaction degrees, and XANES parameters, we have to distinguish two periods for the reaction : the first 14 h and the following period between 30 and 168 h.

XRD patterns show the structural change that affects the aggregate during the reaction. During the first 14 h, we do not observe significant evolutions of the XRD and XANES parameters. The XANES spectrum of the 14-h sample is very close to that of rough flint aggregate. The little variation in the content of the amorphous fraction between rough flint aggregate and the sample after 14 h of attack can be explained by the dissolution phenomenon at the beginning of the reaction according to the reaction degree curve (Fig. 1b). This period corresponds to the formation of Q_0 tetrahedra by dissolution of poorly crystallized fraction present in the aggregate. After 14 h, the formed Q_3 sites remain in the aggregate and their quantity increases with the duration of the attack inducing an increase in the content of the amorphous fraction (Fig. 6). The increase in the amorphous fraction under the effect of the reaction shows that this reaction yields the formation of amorphous products inside the aggregate. This effect could support the phenomenon of swelling of the aggregate within the concrete. In the Figs. 5 and 6 at 168 h, the curve has not reached the asymptote, the quantity of the amorphous fraction keeps increasing, which shows that the reaction is not finished yet.

The origin of the structures of XANES spectrum of c-SiO_2 was largely discussed by Li et al. [14,15]. The A peak in Fig. 7a is due to the transition from the electrons 1 s of silicon towards the 3p-like state. For c-SiO_2, this peak is located at 1847 eV; it is the proof of the presence of silicon in a tetrahedral environment of oxygen and that the electronic structure of silicon remained unchanged. According to Fig. 7a, we can observe that the position of A peak is the same in rough flint aggregate as in c-SiO_2. This shows that silicon atoms in the flint aggregate are in a tetrahedral environment of oxygen. During the reaction, the position of this peak remains the same compared to that of c-SiO_2 and of the flint whatever the duration of attack (Fig. 7b). This means that the tetrahedral environment of silicon is preserved during the reaction. This result is in agreement with the results of the crossed polarization ^{29}Si solid NMR spectroscopy, which shows the existence of a peak at -107 ppm [9] that characterizes the presence of silicon in a tetrahedral environment. The B, C, and D peaks are attributed to multiple scattering in quartz [14,15]; their intensities depend on the evolution of the crystal structure. A study of their evolution in alpha quartz, cristobalite, coesite, opal, and amorphous silica showed that their intensity is cancelled when transforming a crystal structure to an amorphous compound. It was shown that these peaks B, C, and D disappear in amorphous silica. The evolution of the position and the intensity of these peaks can in our case be a good parameter to study the amorphisation of the crystal structure of the aggregate. In our samples (Fig. 7a and b), we notice that the intensity of these peaks decreases with the duration of the reaction especially from 30 to 168 h. This means that until 14 h, the reaction does not affect much the crystal structure of the aggregate. After 30 h, the effect of the reaction is much more appreciable and continuous with the time of attack to an amorphisation of the aggregate. This result is in agreement with the evolution of n^*.

6. Conclusion

The structural evolution of a flint aggregate attacked by alkali–silica reaction has been studied. X-ray diffraction enabled us to determine the percentage of the amorphous fraction and to correlate it to the molar fraction of Q_3 sites

n*. We showed that between 30 and 168 h, the amorphous fraction increases linearly with the number of Q_3 sites. After 168 h, the mechanism of amorphisation is not finished yet. Thanks to Si-K XANES results, we highlighted the amorphisation of this aggregate during the reaction and confirmed the fact that silicon is always present in a tetrahedral environment of oxygen. We also showed that the amorphisation of the aggregate during the reaction is not as simple as the transformation of c-SiO_2 into amorphous silica. The increase in the amorphous fraction under the effect of the reaction shows that the alkali–silica reaction causes the formation of amorphous products inside the aggregate. This effect could support the phenomenon of swelling of the aggregate within the concrete.

The relationship between the evolution of the XANES spectra and n* is planned in a later study by modeling XANES spectra. A study is in hand by EXAFS to quantify the local environment of silicon (type and number of neighbors, interatomic distances) in the aggregate during the reaction. These results are likely to give us information about the role of the modifications on an atomic scale of the aggregate in the phenomenon of swelling.

References

[1] H. Wang, J.E. Gillot, Mechanism of alkali–silica reaction and significance of calcium hydroxide, Cem. Concr. Res. 21 (1991) 647–654.
[2] M. Prezzi, P.J.M. Monteiro, G. Sposito, The alkali–silica reaction: Part 1. Use of the double-layer theory to explain the behavior of reaction-product gels, ACI Mater. J. 94 (1) (1997) 10–17.
[3] D. Bulteel, E. Garcia-Diaz, J. Dürr, L. Khouchaf, C. Vernet, J.M. Siwak, Etude d'un granulat alcali-réactif par diffraction des rayons X, J. Phys. IV (10) (2000) 513–520.
[4] A.B. Poole, Alkali–silica reactivity mechanisms of gel formation and expansion, Proceedings of the 9th International Conference on Alkali-Aggregate Reaction, London (England), vol. 104 (1), Concrete Society Publications CS, 1992, pp. 782–789.
[5] R. Dron, Thermodynamique de la réaction alcali-silice, Bulletin de liaison des Laboratoires des Ponts et Chaussées 166 (1990) 55–59.
[6] S. Diamond, Chemistry and other characteristics of ASR gels, in: M.A. Berube, et al. (Ed.), Proceedings of the 11th International Conference on Alkali-Aggregate Reaction in Concrete, Quebec (Canada), 2000, pp. 31–40.
[7] P. Rivard, J.P. Olivier, G. Balivy, Characterization of the ASR rim application of the Potsdam sandstone, Cem. Concr. Res. 32 (2002) 1259–1267.
[8] D. Bulteel, E. Garcia-Diaz, C. Vernet, H. Zanni, Alkali–silica reaction: a method to quantify the reaction degree, Cem. Concr. Res. 32 (2002) 1199–1206.
[9] D.Bulteel, Quantification de la reaction alcali-silice : application à un silex du nord de la FRANCE, Thèse de doctorat de l'Université des Sciences et Techniques de Lille (2000).
[10] Ph. Sainctacvit, J. Petiau, C. Laffon, A.-M. Flank, P. Lagarde, S.S. Hasnain, in: S. S. Hasnain (Ed.), X-Ray Absorption Fine Structure, Ellis Horwood, New York, 1991, pp. 38–40.
[11] P. Lagarde, A.-M. Flank, J.-P. Itié, Polarized XANES spectra of quartz: application to the structure of densified silica, Jpn. J. Appl. Phys. 32 (1993) 613–615.
[12] L. Beck, M. Gehlen, A.M. Flank, A.J. Van Bennekom, J.E.E. Van Beusekom, The relationship between Al and Si in biogenic silica as determined by PIXE and XAS, Beam Interactions with Materials and Atoms (2002).
[13] K.E. Kurtis, F.A. Rodrigues, P.J.M. Monteiro, J.T. Brown, The alkali-silica reaction: (I) surface charge measurements and (II) in-situ observations by X-ray microscopy, Proceedings of the Second International Conference on Concrete Under Severe Conditions: Environment and Loading, CONSEC, Tromsø, Norway, June (1998) 317–326.
[14] D. Li, et al., High-resolution Si K and $L_{2,3}$ edge XANES of α-quartz and sishtovite, Solid State Commun. 87 (1993) 613–617.
[15] D. Li, et al., X-ray absorption of silicon dioxide (SiO2) polymorphs: the structural characterization of opal, Am. Mineral. 79 (1994) 622–632.
[16] C. Levelut, D. Cabaret, M. Benoit, P. Jund, A.-M. Flanck, Multiple scattering calculations of the XANES Si K-edge in amorphous silica, J. Non-Cryst. Solids 293–295 (2001) 100–104.
[17] L.S. Dent Glasser, N. Kataoka, The chemistry of alkali-aggregate reaction, Proceedings of the 5th International Conference on Alkali–Aggregate Reaction, National Building Research Institute of the CSIR, Cape Town, South Africa, 1981, p. 7 (Paper S252/23).
[18] S. Chatterji, N. Thaulow, Some fundamental aspects of alkali silica reaction, in: M.A. Bérubé, B. Fournier, B. Durand (Eds.), Proceedings of the 11th International Conference on Alkali–Aggregate Reaction in Concrete Quebec (Canada), 2000, pp. 21–29.
[19] R.K. Iler, The Chemistry of Silica, Wiley, New York, 1979.
[20] P. Caussin, J. Nusinovici, D.W. Beard, Using digitized X-ray powder diffraction scans as input for a new PC-At search/match program, Adv. X-ray Anal. 31 (1988) 423–430.